

compounds, as well as to produce entirely new compounds such as californium monoxide. Leger and co-workers have already employed pressure-induced reactions to synthesize some lanthanide monoxides.⁸ Further work in our laboratory will explore these possibilities along with increasing our understanding of the effects of pressure, as observed by changes in the optical absorption spectra, on actinide halides.

Acknowledgment. The californium-249 used in this work was made available by the Division of Chemical Sciences, U.S. Department of Energy, through the transplutonium element production facilities at the Oak Ridge National Laboratory. The research was sponsored by the Division of Chemical Sciences, U.S. Department of Energy, partly under contract DE-AS05-76ER04447 with the University of Tennessee, Knoxville (J.R.P.,

J.P.Y., U.B.), and partly under contract DE-AC05-84OR21400 with Martin Marietta Energy Systems, Inc. (R.G.H., G.M.B.).

Registry No. CfBr₃, 20758-68-3.

Department of Chemistry
University of Tennessee
Knoxville, Tennessee 37996-1600

J. R. Peterson^{*9}

Analytical Chemistry and Chemistry Divisions
Transuranium Research Laboratory
Oak Ridge National Laboratory
Oak Ridge, Tennessee 37831

J. P. Young^{10a}
R. G. Haire^{10b}
G. M. Begun^{10b}

Commission of the European Communities
Joint Research Centre
European Institute for Transuranium
Elements
Karlsruhe, Federal Republic of Germany

U. Benedict

- (8) Leger, J. M.; Yacoubi, N.; Lories, J. "The Rare Earths in Modern Science and Technology"; McCarthy, G. J., Rhyne, J. J., Silber, H. B., Eds.; Plenum Press: New York, 1980; Vol. II, p 203.
(9) Also affiliated with the Chemistry Division, Oak Ridge National Laboratory.
(10) (a) Analytical Chemistry Division. (b) Chemistry Division.

Received March 15, 1985

Articles

Contribution from the Laboratory of Analytical Chemistry, Faculty of Science, Nagoya University, Chikusa, Nagoya 464, Japan, and Faculty of Pharmacy, Meijo University, Tempaku, Nagoya 466, Japan

Equilibria and Kinetics of the Reactions of Water-Soluble Molybdenum(V) Porphyrins with Hydrogen Peroxide in Aqueous Solutions¹

MASAHIKO INAMO,^{2a} SHIGENOBU FUNAHASHI,^{2a} YOSHIO ITO,^{2b} YOSHIKI HAMADA,^{2b} and MOTOHARU TANAKA^{*2a}

Received January 2, 1985

Equilibria of (5,10,15,20-tetrakis(4-*N*-methylpyridiniumyl)porphine(2+))oxomolybdenum(V) (Mo(V)-TMPyP complex) and its reaction with hydrogen peroxide have been investigated in aqueous solutions at $I = 1.00$ M by ESR and visible spectroscopies. The Mo(V)-TMPyP complex hydrolyzes and dimerizes to give rise to the following four species: $[\text{Mo}^{\text{VO}}(\text{tmpyp})\text{OH}]^{4+}$ (1), $[\text{Mo}^{\text{VO}}(\text{tmpyp})\text{OH}]^{4+}$ (2), the bis(μ -hydroxo) dimer $[(\text{tmpyp})\text{OMo}^{\text{VO}}(\mu\text{-OH})_2\text{Mo}^{\text{VO}}(\text{tmpyp})]^{8+}$ (3), and the (μ -hydroxo)(μ -oxo) dimer $[(\text{tmpyp})\text{OMo}^{\text{VO}}(\mu\text{-O})(\mu\text{-OH})\text{Mo}^{\text{VO}}(\text{tmpyp})]^{7+}$ (4). Equilibrium constants were obtained to be $K_{a1} = [2][\text{H}^+][1]^{-1} = 10^{-7.18 \pm 0.02}$ M, $K_{a2} = [4][\text{H}^+][3]^{-1} = 10^{-10.0 \pm 0.1}$ M, and $K_D = [3][2]^{-2} = 10^{6.00 \pm 0.05}$ M⁻¹ at 25 °C. The rate law for the dissociation of dimer 3 to give monomers 1 and 2 is $-d[3]/dt = k_d[3][\text{H}^+]$ with $k_d = (4.1 \pm 0.2) \times 10^4$ M⁻¹ s⁻¹ at 25 °C over the pH range 7.1-7.6. The reaction of the Mo(V)-TMPyP complex with hydrogen peroxide gives three types of peroxo complexes. Over the pH range 5-8 the peroxomolybdenum(V) complex $[\text{Mo}^{\text{VO}}(\text{O}_2)(\text{tmpyp})]^{3+}$ (5) was obtained, while in acidic aqueous solution 1 is oxidized by hydrogen peroxide to produce $[\text{Mo}^{\text{VI}}(\text{O}_2)(\text{tmpyp})\text{OH}]^{6+}$ (6). The substitution of the coordinated water molecule in 6 by hydrogen peroxide yielded a third type of the peroxo complex, $[\text{Mo}^{\text{VI}}(\text{O}_2)_2(\text{tmpyp})]^{4+}$ (7). Formation constants of 5 and 7 were determined to be $K_{\text{Mo(V)}} = [5][\text{H}^+]^2[1]^{-1}[\text{H}_2\text{O}_2]^{-1} = 10^{-9.02 \pm 0.03}$ M and $K_{\text{Mo(VI)}} = [7][\text{H}^+]^2[6]^{-1}[\text{H}_2\text{O}_2]^{-1} = 10^{-8.16 \pm 0.03}$ M, respectively, at 25 °C. The formation of 6 is second order with respect to the concentration of hydrogen peroxide and first order with respect to that of 1, and activation parameters were estimated as follows: $k_{\text{TMPyP}}(25 \text{ }^\circ\text{C}) = 3.27 \times 10^{-4}$ M⁻² s⁻¹, $\Delta H^\ddagger = 74 \pm 1$ kJ mol⁻¹, $\Delta S^\ddagger = -63 \pm 3$ J K⁻¹ mol⁻¹, $\Delta V^\ddagger = 1.3 \pm 0.3$ cm³ mol⁻¹. The mechanism of formation of 5 from 1 and H₂O₂ includes a pre-equilibrium hydrolysis of 1, followed by the rate-determining substitution. Activation parameters for the latter are $k_f(25 \text{ }^\circ\text{C}) = 1.05 \times 10^3$ M⁻¹ s⁻¹, $\Delta H^\ddagger = 37 \pm 1$ kJ mol⁻¹, $\Delta S^\ddagger = -63 \pm 3$ J K⁻¹ mol⁻¹, and $\Delta V^\ddagger = -0.2 \pm 0.3$ cm³ mol⁻¹. An interchange mechanism is most probably operative in this reaction.

Introduction

In recent years the chemistry of molybdenum porphyrins has been extensively investigated. Studies include the synthesis, structural characterization, and chemical reactivities of their dioxygen complexes.³⁻⁶ Complexes of early transition metals in

high oxidation state have been known to react with hydrogen peroxide to produce peroxo complexes. Molybdenum(V) porphyrins give rise to the corresponding peroxomolybdenum(VI) complexes in organic media. Chevrier et al. first reported on the synthesis and crystal structure of diperoxomolybdenum(VI) porphyrin, Mo^{VI}(O₂)₂(tptp).^{3,7} Photochemical⁴ and electro-

- (1) Reactions of Hydrogen Peroxide with Metal Complexes. 8. Preliminary communication: Inamo, M.; Funahashi, S.; Ito, Y.; Hamada, Y.; Tanaka, M. *Chem. Lett.* **1985**, 19. Part 7: Inamo, M.; Funahashi, S.; Tanaka, M. *Inorg. Chem.* **1983**, 22, 3734.
(2) (a) Nagoya University. (b) Meijo University.
(3) Chevrier, B.; Diebold, T.; Weiss, R. *Inorg. Chim. Acta* **1976**, 19, L57.
(4) Ledon, H.; Bonnet, M.; Lallemand, J.-Y. *J. Chem. Soc., Chem. Commun.* **1979**, 702. Ledon, H. J.; Bonnet, M.; Galland, D. *J. Am. Chem. Soc.* **1981**, 103, 6209.

- (5) Kadish, K. M.; Cheng, D.; Malinski, T.; Ledon, H. *Inorg. Chem.* **1983**, 22, 3490.
(6) Imamura, T.; Hasegawa, K.; Fujimoto, M. *Chem. Lett.* **1983**, 705.
(7) Ligand abbreviations: H₂tptp, 5,10,15,20-tetra-*p*-tolylporphine (TpTP); H₂tpp, 5,10,15,20-tetraphenylporphine; H₂tpyp, 5,10,15,20-tetra-4-pyridylporphine (TPyP); H₂tmpyp, 5,10,15,20-tetrakis(4-*N*-methylpyridiniumyl)porphine(4+) (TMPyP); H₂ttmp, 5,10,15,20-tetra-*m*-tolylporphine (TmTP); H₂tpps, 5,10,15,20-tetrakis(4-sulfonatophenyl)porphine (TPPS).

chemical⁵ behavior of this type of peroxo complex has been also studied. A different type of peroxomolybdenum porphyrin, $\text{Mo}^{\text{V}}\text{O}(\text{O}_2)(\text{tpp})$,⁷ has been obtained by the reaction of the corresponding molybdenum(V) porphyrin with superoxide ion in organic media.⁶

In this paper we describe the reaction of water-soluble molybdenum(V) porphyrins (5,10,15,20-tetrakis(4-*N*-methylpyridiniumyl)porphine(2+))oxomolybdenum(V) ($\text{Mo}(\text{V})\text{-TMPyP}$ complex) and oxo(5,10,15,20-tetra-4-pyridylporphinato(2-))molybdenum(V) ($\text{Mo}(\text{V})\text{-TPyP}$ complex) with hydrogen peroxide in aqueous solutions. Solution equilibria of the complexes necessary for the present purpose are also described.

Experimental Section

Reagents. Reagent grade sodium nitrate (Wako Pure Chemical Industries, Ltd., Osaka, Japan) was recrystallized twice from distilled water. Nitric acid of special purity (Wako) was used without further purification. The 60% hydrogen peroxide solution containing no stabilizing agent (donated from Mitsubishi Gas Chemical Co. Inc., Kanagawa, Japan) was purified by distillation under reduced pressure. A solution of hydrogen peroxide was titrated with a standard solution of potassium permanganate. MES (2-morpholinoethanesulfonic acid) and MOPS (3-morpholinopropanesulfonic acid) (Wako) used as pH buffers were recrystallized twice from aqueous ethanol.

Hydroxooxo(5,10,15,20-tetra-4-pyridylporphinato(2-))molybdenum(V), $\text{Mo}^{\text{V}}\text{O}(\text{tpp})\text{OH}$,⁷ was prepared as follows: A 1.0-g portion of 5,10,15,20-tetra-4-pyridylporphine (H_2tpp) (Strem Chemicals) and a 16-g portion of anhydrous sodium carbonate were dissolved in 250 cm³ of phenol. Under an argon atmosphere a 6.0-g portion of molybdenum pentachloride was added to the reaction mixture. The solution was kept at 180–190 °C with stirring for 15 h. The solution was mixed with chloroform and filtered. The filtrate was washed with a 2.5 M⁸ aqueous solution of sodium hydroxide. The product was then extracted into the 3 M hydrochloric acid solution. After neutralization of the aqueous solution with sodium carbonate, the product was extracted again into chloroform. After the solution was evaporated to dryness, the residue was dissolved in chloroform and then subjected to column chromatography (neutral aluminum oxide, Woelm, activity grade 1). A dark green band was eluted with chloroform. Recrystallization from a mixture of chloroform and methanol (1:9 v/v) gave dark violet crystals. Anal. Calcd for $\text{C}_{40}\text{H}_{25}\text{MoN}_8\text{O}_2$: C, 64.43; H, 3.38; N, 15.03. Found: C, 64.07; H, 3.68; N, 13.76. Hydroxooxo(5,10,15,20-tetrakis(4-*N*-methylpyridiniumyl)porphine(2+))molybdenum(V) iodide, $[\text{Mo}^{\text{V}}\text{O}(\text{tmpyp})\text{OH}]\text{I}_4$,⁷ was obtained by the following procedure. A 30-mg portion of $\text{Mo}^{\text{V}}\text{O}(\text{tpp})\text{OH}$ and a large excess of methyl iodide (3 cm³) were dissolved in the mixture of methanol–acetone (1:9 v/v) in a standard reflux apparatus. The mixture was kept at 60 °C for 3 h. The methylated metalloporphyrin that precipitated was collected on a funnel. Anal. Calcd for $\text{C}_{44}\text{H}_{40}\text{I}_4\text{MoN}_8\text{O}_3$ (monohydrate): C, 39.69; H, 2.95; N, 8.42. Found: C, 39.48; H, 2.84; N, 8.30.

Measurement. Temperature of the reaction solution was controlled to within ± 0.1 °C with a thermoelectric circulating bath. The ionic strength was adjusted to 1.00 M with sodium nitrate and nitric acid. The hydrogen ion concentration was determined by an Orion Research pH meter (Model 701A) with a glass electrode (Metrohm, Type EA109) and a reference electrode (Metrohm, Type EA404) when pH was higher than 2.0. A 1.000×10^{-2} M nitric acid solution of $I = 1.00$ M was used as a pH standard solution. Visible absorption spectra were recorded on a highly sensitive spectrophotometer (Type SM401, Union Giken, Osaka, Japan). ESR spectra were obtained on a JEOL ES-SCXA X-band spectrometer. A standard Mn(II)/MgO sample was employed for the calibration of the magnetic field.

In all kinetic measurements, reactions were followed spectrophotometrically. When the reaction was fast, a stopped-flow spectrophotometer (Type RA401, Union Giken) was used to obtain the kinetic data. The progress of reactions under various pressures up to 180 MPa was measured with a high-pressure stopped-flow apparatus exploited in our laboratory⁹ or with a high-pressure cell connected to a spectrophotometer.

Results

Equilibria of the $\text{Mo}(\text{V})\text{-TMPyP}$ Complex in Aqueous Solutions. The $\text{Mo}(\text{V})\text{-TMPyP}$ complex, $[\text{Mo}^{\text{V}}\text{O}(\text{tmpyp})\text{OH}]\text{I}_4$, is soluble in aqueous solution over an entire pH range. Apparent molar absorption coefficients, $\bar{\epsilon}$, of the $\text{Mo}(\text{V})\text{-TMPyP}$ complex

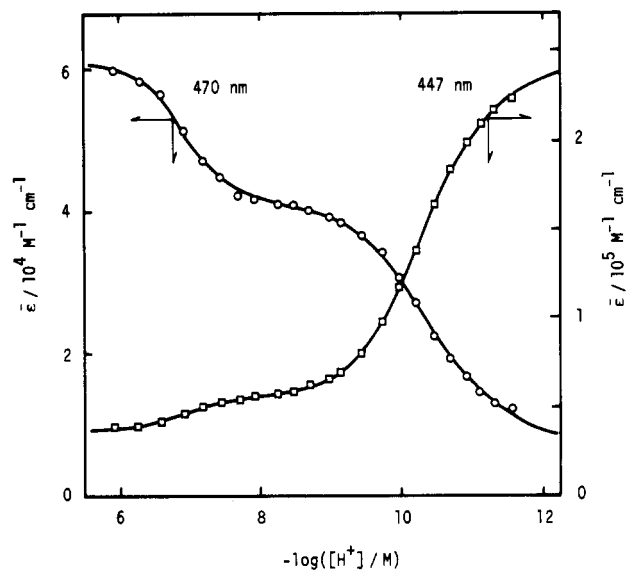


Figure 1. Spectrophotometric titration of the $\text{Mo}(\text{V})\text{-TMPyP}$ complex at 25 °C and $I = 1.00$ M (NaNO_3). The total concentration of the $\text{Mo}(\text{V})\text{-TMPyP}$ complex, $C_{\text{Mo}(\text{V})\text{-TMPyP}}$, is 5.29×10^{-6} M. Solid lines are computer fits of the data to eq 1.

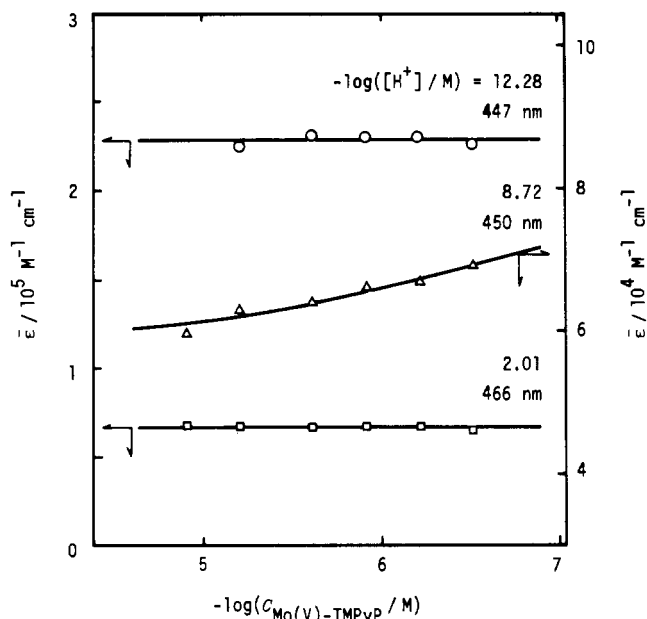
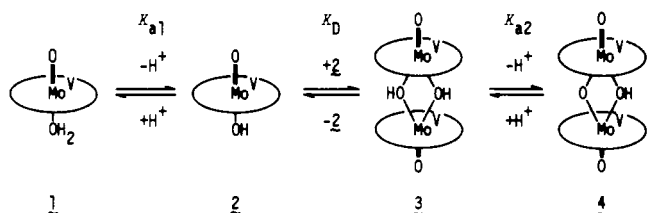


Figure 2. Plots of $\bar{\epsilon}$ vs. $-\log(C_{\text{Mo}(\text{V})\text{-TMPyP}}/M)$ at 25 °C. Solid lines are calculated by the obtained values.

Scheme I



at 447 and 470 nm are plotted against $-\log([H^+]/M)$ in Figure 1. Figure 2 shows the dependence of $\bar{\epsilon}$ values on the total concentration of the complex ($C_{\text{Mo}(\text{V})\text{-TMPyP}}$ per molybdenum atom in M). In both the acidic and basic aqueous solutions the $\bar{\epsilon}$ values are constant, while over the intermediate pH range the values at 450 nm increase with the decrease of the total concentration of the complex. This points to the equilibrium between the monomeric and dimeric species. From Figures 1 and 2 we propose the equilibrium network of the $\text{Mo}(\text{V})\text{-TMPyP}$ complex in aqueous solution as shown in Scheme I. Equilibrium constants

(8) 1 M = 1 mol dm⁻³.

(9) Ishihara, K.; Funahashi, S.; Tanaka, M. *Rev. Sci. Instrum.* **1982**, *53*, 1231.

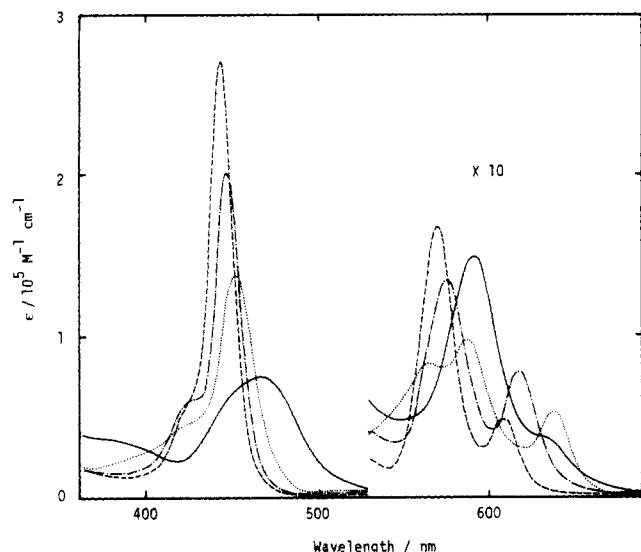


Figure 3. Visible absorption spectra of **1** (—), **5** (···), **6** (---), and **7** (-·-·).

in Scheme I are defined as follows: $K_{a1} = [2][H^+][1]^{-1}$, $K_{a2} = [4][H^+][3]^{-1}$, and $K_D = [3][2]^{-2}$. The values of K_{a1} and K_D can also be determined by the kinetic experiments (vide infra). With a knowledge of the K_{a1} and K_D values obtained from the kinetic data the value of K_{a2} was evaluated by applying the nonlinear least-squares fit to the results shown in Figure 1 according to eq 1,¹⁰ where ϵ_1 , ϵ_2 , ϵ_3 , and ϵ_4 are the molar absorption coefficients

$$\bar{\epsilon}C_{\text{Mo(V)-TMPyP}} = \epsilon_1[1] + \epsilon_2[2] + \epsilon_3[3] + \epsilon_4[4] \quad (1)$$

of species **1**–**4**, respectively, at a given wavelength. We have $K_{a1} = (6.6 \pm 0.3) \times 10^{-8}$ M, $K_{a2} = (1.0 \pm 0.2) \times 10^{-10}$ M, and $K_D = (1.0 \pm 0.1) \times 10^6$ M⁻¹ at 25 °C. The solid lines in Figures 1 and 2 were computed by using the obtained values.

An ESR spectrum of **1** in the acidic media at room temperature displays the typical feature for the molybdenum(V) porphyrin complexes previously reported,^{11,12} which consists of nine intense lines at the center and six weaker bands in a wider range as demonstrated in Figure S1 (supplementary material). The g value of 1.969 is very close to those of Mo^VO(tpp)X complexes in the organic solvent (X = a monodentate ligand such as hydroxide, alkoxide, or halide).

Reaction of the Mo(V)–TMPyP Complex with H₂O₂ in Neutral Aqueous Solution. Visible and ESR spectroscopies were used to monitor the reaction of the Mo(V)–TMPyP complex with hydrogen peroxide. The ESR spectrum of the reaction product at room temperature is characteristic of the pentavalent molybdenum complex with a g value of 1.970 as depicted in Figure S1, though the superhyperfine structure at the central intense absorption due to the interactions with four nitrogen nuclei of the porphyrin cannot be observed under our experimental conditions as was the case for [Mo^V(O₂)₂(tmp)]⁻.^{5,7} Over the pH range 5–6 the visible absorption spectra of the complex solutions containing various amount of hydrogen peroxide exhibit the clear isosbestic points at 394, 469, and 529 nm. The change in the visible absorption spectra is ascribed to the formation of the 1:1 peroxo complex. The conditional formation constant $K'_{\text{Mo(V)}}$ was estimated at various hydrogen ion concentrations: $K'_{\text{Mo(V)}} = [1:1 \text{ peroxo}$

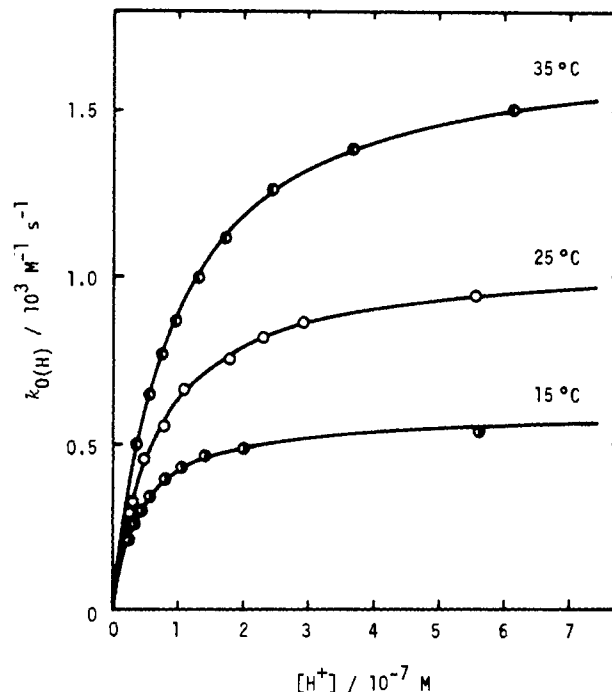


Figure 4. Dependence of the second-order rate constant, $k_{0(H)}$, for the formation reaction of **5** on the hydrogen ion concentration. MOPS was used as a pH buffer ($C_{\text{MOPS}} = 2.40 \times 10^{-3}$ M). Each point is the average of several runs. Solid lines are calculated by using the activation parameters obtained.

Table I. Values of k_f and K_{a1} at Various Temperatures

$T/^\circ\text{C}$	$10^{-3}k_f/\text{M}^{-1}\text{s}^{-1}$	$10^8K_{a1}/\text{M}$
15	0.590	4.10
25	1.05	6.58
35	1.71	9.16

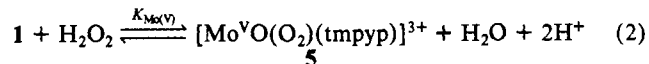
$$\Delta H_f^\ddagger = 37 \pm 1 \text{ kJ mol}^{-1}$$

$$\Delta S_f^\ddagger = -63 \pm 3 \text{ J K}^{-1} \text{ mol}^{-1}$$

$$\Delta H(K_{a1}) = 30 \pm 3 \text{ kJ mol}^{-1}$$

$$\Delta S(K_{a1}) = -38 \pm 7 \text{ J K}^{-1} \text{ mol}^{-1}$$

complex][1]⁻¹[H₂O₂]⁻¹ = $(3.7 \pm 0.5) \times 10$ M⁻¹ at $[H^+] = 5.04 \times 10^{-6}$ M, $(1.15 \pm 0.05) \times 10^2$ M⁻¹ at $[H^+] = 2.93 \times 10^{-6}$ M (Figure S2, supplementary material), and $(2.25 \pm 0.09) \times 10^2$ M⁻¹ at $[H^+] = 2.06 \times 10^{-6}$ M. The plot of $\log(K'_{\text{Mo(V)}}/\text{M}^{-1})$ against $-\log([H^+]/\text{M})$ gave a straight line with a slope of 2 (the inset in Figure S2), which is consistent with the release of two protons in this peroxo complex formation. Therefore, the reaction is expressed by eq 2. The constant for eq 2 was determined to be $K_{\text{Mo(V)}} = [5][H^+]^2[1]^{-1}[H_2O_2]^{-1} = (9.6 \pm 0.7) \times 10^{-10}$ M at 25 °C. In Figure 3 visible absorption spectra of **1** and **5** are depicted.



Kinetics of peroxo complex formation by the reaction of the Mo(V)–TMPyP complex with hydrogen peroxide was studied spectrophotometrically over the pH range from 5.2 to 7.6 where species **1**–**3** exist. In all kinetic experiments hydrogen peroxide was used in a large excess over the Mo(V)–TMPyP complex. The peroxo complex formation was found to involve fast and slow reactions. The change in absorbance at 454 nm in those reactions, i.e., the production of **5**, depends on pH. The contribution of the faster reaction to the total absorbance change decreases with increasing pH and is related to the proportion of monomeric species, **1** and **2**, and the dimeric species, **3**: the faster reaction is attributable to the reaction of the monomers, while the slower reaction corresponds to that of the dimer as discussed later.

First of all, we shall describe the fast reaction. First-order plots are linear at least for 3 half-lives. The conditional first-order rate

(10) The following equations were solved simultaneously for K_{a2} : $\bar{\epsilon}C_{\text{Mo(V)-TMPyP}} = (\epsilon_1 + \epsilon_2K_{a1}[H^+]^{-1})[1] + K_{a1}^2K_D[H^+]^{-2}(\epsilon_3 + \epsilon_4K_{a2}^{-1}[H^+]^{-1})[1]^2$; $C_{\text{Mo(V)-TMPyP}} = (1 + K_{a1}[H^+]^{-1})[1] + 2K_{a1}^2K_D[H^+]^{-2}(1 + K_{a2}[H^+]^{-1})[1]^2$.

(11) Srivastava, T. S.; Fleischer, E. B. *J. Am. Chem. Soc.* **1970**, *92*, 5518. Fleischer, E. B.; Srivastava, T. S. *Inorg. Chim. Acta* **1971**, *5*, 151. Newton, C. M.; Davis, D. G. *J. Magn. Reson.* **1975**, *20*, 446. Bains, M. S.; Davis, D. G. *Inorg. Chim. Acta* **1979**, *37*, 53. Imamura, T.; Terui, M.; Takahashi, Y.; Numatatsu, T.; Fujimoto, M. *Chem. Lett.* **1980**, 89. Ledon, H. J.; Bonnet, M. C.; Brigandat, Y.; Varescon, F. *Inorg. Chem.* **1980**, *19*, 3488.

(12) Matsuda, Y.; Kubota, F.; Murakami, Y. *Chem. Lett.* **1977**, 1281.

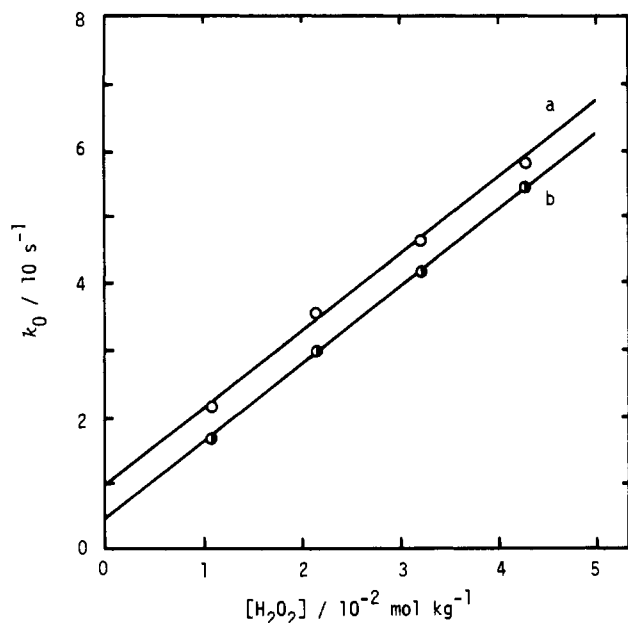


Figure 5. Dependence of the first-order rate constant, k_0 , for the formation reaction of **5** on the concentration of hydrogen peroxide at 25 °C and $-\log ([\text{H}^+]/\text{mol kg}^{-1}) = 5.408$ (at 0.1 MPa) at constant pressure: (a) 0.1 MPa; (b) 117.6 MPa. Each point is the average of several determinations.

constants, k_0 , are linearly related to the hydrogen peroxide concentration at constant acidity. The conditional second-order rate constant, $k_{0(\text{H})}$, depends on the hydrogen ion concentration (Figure 4). The results given in Figure 4 were obtained under conditions where the reverse reaction was practically negligible ($-\log ([\text{H}^+]/\text{M}) > 6.3$ and $[\text{H}_2\text{O}_2] > 0.01 \text{ M}$). $k_{0(\text{H})}$ is well fitted to the function $k_{0(\text{H})} = k_f(1 + K_{a1}[\text{H}^+]^{-1})^{-1}$, as shown by the solid lines in Figure 4. This equation is consistent with the reaction scheme including the preequilibrium hydrolysis of **1**. Thus, the rate law is expressed as

$$d[\mathbf{5}]/dt = k_f(1 + K_{a1}[\text{H}^+]^{-1})^{-1}([\mathbf{1}] + [\mathbf{2}])[\text{H}_2\text{O}_2] \quad (3)$$

Values of k_f and K_{a1} at different temperatures are tabulated in Table I.

According to the transition-state theory the change in rate constant, k , with pressure, P , is related to the activation volume ΔV^\ddagger : $(\partial \ln k / \partial P)_T = -\Delta V^\ddagger / RT$. Rate constants at various pressures up to 180 MPa were determined at $-\log ([\text{H}^+]/\text{mol kg}^{-1}) = 5.408$ (at 0.1 MPa) where the reverse reaction was not negligible. In Figure 5 is shown the dependence of the conditional first-order rate constant, k_0 , on the concentration of hydrogen peroxide at 0.1 and 117.6 MPa. The slope and the intercept of the straight line in Figure 5 correspond to the second-order rate constant of the forward reaction, k_f , and the conditional first-order rate constant of the reverse reaction, k'_b , respectively.¹³ k'_b was kinetically confirmed to be expressed as $k_b[\text{H}^+]^2$, and we obtained $k_b = 0.68 \times 10^{12} \text{ M}^{-2} \text{ s}^{-1}$ at 0.1 MPa and 25 °C. This is in accord with the third-order rate constant k_b obtained from the relation $k_b = k_f K_{\text{Mo(V)}}^{-1}$ by using the values of k_f and $K_{\text{Mo(V)}}$ obtained above: $k_b = (1.1 \pm 0.1) \times 10^{12} \text{ M}^{-2} \text{ s}^{-1}$ at 25 °C.

Figure 6 shows the pressure dependence of k_f and k'_b at 25 °C. Hydrogen ion concentration was adjusted by using MES as a pH buffer. Since the plot is linear within the experimental uncertainty for both cases, the activation volume is assumed to be pressure independent. The hydrogen ion concentration of the sample solution should decrease with increasing pressure because the volume change for the proton dissociation of MES is, $\Delta V = 5.0 \text{ cm}^3 \text{ mol}^{-1}$.¹⁴ Under the present conditions the change in pH with

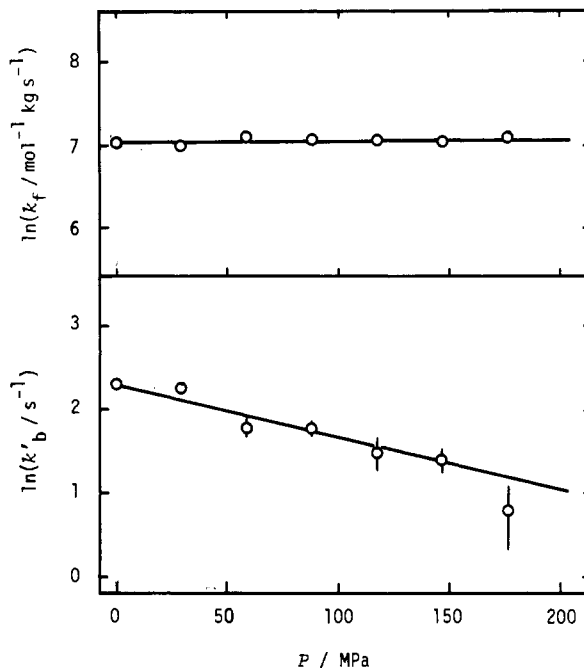


Figure 6. Pressure dependence of k_f and k'_b at 25 °C.

pressure is equal to the change of $\text{p}K_a$ of MES.¹⁵ Taking into account this pressure effect, we have the following activation volumes: $\Delta V_f^\ddagger = -0.2 \pm 0.3 \text{ cm}^3 \text{ mol}^{-1}$ and $\Delta V_b^\ddagger = 5.2 \pm 1.6 \text{ cm}^3 \text{ mol}^{-1}$ at 25 °C and $I = 1.05 \text{ mol kg}^{-1}$. Values of the rate constants at zero pressure obtained from the intercept in Figure 6 are in agreement with those obtained by a conventional method at atmospheric pressure.

Now we shall turn to the slow reaction, i.e., the reaction of the dimeric species **3**. The formation of the peroxo complex **5** from **3** reacting with hydrogen peroxide is first order with respect to the concentration of **3**, while it is independent of the concentration of hydrogen peroxide. First-order rate constants were determined to be $(1.16 \pm 0.06) \times 10^{-3} \text{ s}^{-1}$ at $[\text{H}^+] = 2.61 \times 10^{-8} \text{ M}$ and $(3.17 \pm 0.14) \times 10^{-3} \text{ s}^{-1}$ at $[\text{H}^+] = 7.73 \times 10^{-8} \text{ M}$. The rate law is thus given by eq 4. The second-order rate constant k_d was obtained

$$-d[\mathbf{3}]/dt = \frac{1}{2}d[\mathbf{5}]/dt = k_d[\text{H}^+][\mathbf{3}] \quad (4)$$

to be $(4.1 \pm 0.2) \times 10^4 \text{ M}^{-1} \text{ s}^{-1}$ at 25 °C. The rate-determining step of the slow reaction should be the proton-assisted dissociation of the dimeric species, **3**, to the monomeric species, **2** or **1**. The reaction consists of the fast and slow processes as described above, since the dissociation of the dimer is slow as compared to the reaction of **1** with hydrogen peroxide.

The hydrogen ion concentration dependence of the fast reaction leading to **5** was monitored at 454 nm (the wavelength of the maximum absorption in the Soret region of **5**) over the pH range 6.3–7.6, where the concentration of the dimeric species **4** and the reverse reaction can be neglected. The fraction of the peroxo complex **5** produced by the fast reaction is denoted by R (eq 5),

$$R = \frac{(\epsilon_5 - \epsilon_1)[\mathbf{1}] + (\epsilon_5 - \epsilon_2)[\mathbf{2}]}{(\epsilon_5 - \epsilon_1)[\mathbf{1}] + (\epsilon_5 - \epsilon_2)[\mathbf{2}] + (2\epsilon_5 - \epsilon_3)[\mathbf{3}]} \quad (5)$$

where ϵ_5 refers to the molar absorption coefficient of **5**. R values are plotted against $-\log ([\text{H}^+]/\text{M})$ in Figure 7. With the known values of ϵ_1 – ϵ_3 and ϵ_5 and the K_{a1} value obtained from the kinetic data, the K_D value was evaluated from the data shown in Figure 7:¹⁶ $K_D = (1.0 \pm 0.1) \times 10^6 \text{ M}^{-1}$.

(13) At $-\log ([\text{H}^+]/\text{mol kg}^{-1}) = 5.408$, k_0 for the formation reaction of **5** (eq 2) is expressed as $k_0 = k_f(1 + K_{a1}[\text{H}^+]^{-1})^{-1}[\text{H}_2\text{O}_2] + k'_b \approx k_f[\text{H}_2\text{O}_2] + k'_b$.

(14) Ise, N.; Kunugi, S. *Kagaku Zokan (Kyoto)* **1981**, No. 89, 55.

(15) The total concentration of MES was $3.33 \times 10^{-3} \text{ mol kg}^{-1}$ throughout. Because the solution is well buffered by MES, the pH of the solution is written as $\text{pH} = \text{p}K_a(\text{MES}) + \log ([\text{mes}^-]/[\text{Hmes}])$, where mes^- and Hmes represent a deprotonated species and a neutral form of MES, respectively. Values of $\log ([\text{mes}^-]/[\text{Hmes}])$ were presumed not to vary with increase in pressure up to 180 MPa under the present experimental conditions.

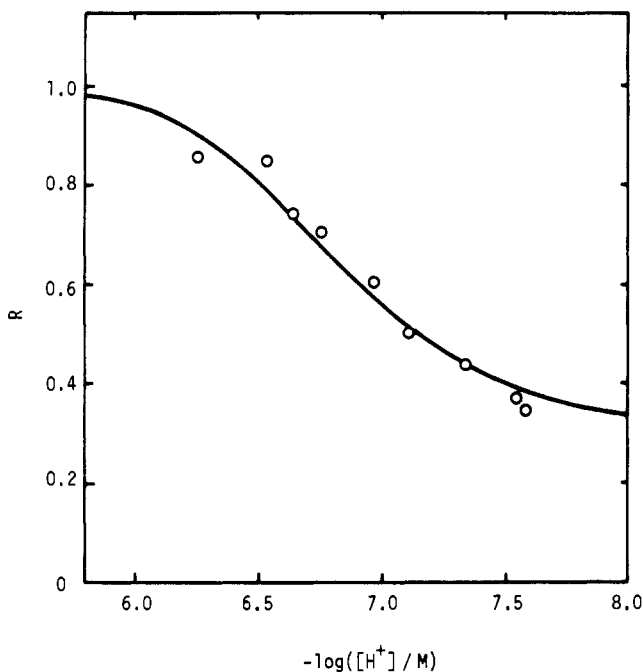


Figure 7. Plots of R values vs. $-\log([H^+]/M)$ at 25 °C and $C_{\text{Mo(V)-TMPyP}} = 6.68 \times 10^{-6} \text{ M}$. The solid line is the computer fit of the data to eq 5.

Table II. Values of k_{TMPyP} and k_{TPyP} at Various Temperatures and Pressures

$T/^\circ\text{C}$	P/MPa	$10^4 k_{\text{TMPyP}}/\text{M}^{-2} \text{s}^{-1}$	$10^4 k_{\text{TPyP}}/\text{M}^{-2} \text{s}^{-1}$
15	0.1	1.11	1.48
25	0.1	3.27	4.47
30	0.1	5.29	7.93
35	0.1	8.91	12.9

$T/^\circ\text{C}$	P/MPa	$10^4 k_{\text{TMPyP}}/\text{mol}^{-2} \text{kg}^{-2} \text{s}^{-1}$	$10^3 k_{\text{TPyP}}/\text{mol}^{-2} \text{kg}^{-2} \text{s}^{-1}$
35	0.1	8.36	1.40
35	24.5	8.11	1.35
35	49.0	7.94	1.28
35	73.5	7.82	1.21
35	98.0	7.88	1.15
35	122.5	7.76	1.14

	TMPyP	TPyP
$\Delta H^\ddagger/\text{kJ mol}^{-1}$	74 ± 1	78 ± 1
$\Delta S^\ddagger/\text{J K}^{-1} \text{mol}^{-1}$	-63 ± 3	-48 ± 3
$\Delta V^\ddagger/\text{cm}^3 \text{mol}^{-1}$	1.3 ± 0.3	4.7 ± 0.4

Reactions of the Mo(V)-TMPyP Complex with H_2O_2 in Acidic Aqueous Solutions. Reactions of the Mo(V)-TMPyP complex with hydrogen peroxide were examined over the pH range 1–3. As the reaction of 1 with hydrogen peroxide proceeds, ESR signals of the molybdenum(V) species gradually decrease and finally disappear. The ESR silence of the reaction product indicates that the molybdenum(V) porphyrin complex is oxidized by hydrogen peroxide to the molybdenum(VI) species with no d electron. A similar oxidation was reported for the reaction of the Mo(V)-TpTP complex with hydrogen peroxide in dichloromethane.³ The reaction was followed by the change of visible absorption spectra with time in the presence of a large excess of hydrogen peroxide. The first-order rate constant, k_0 , is plotted vs. the concentration of hydrogen peroxide in Figure 8. The second-order dependence of these reaction rates on the concentration of hydrogen peroxide leads to the rate law (6). The third-order rate constant k_{TMPyP}

$$-d[1]/dt = k_{\text{TMPyP}}[1][\text{H}_2\text{O}_2]^2 \quad (6)$$

does not depend on the hydrogen ion concentration at $[H^+] =$

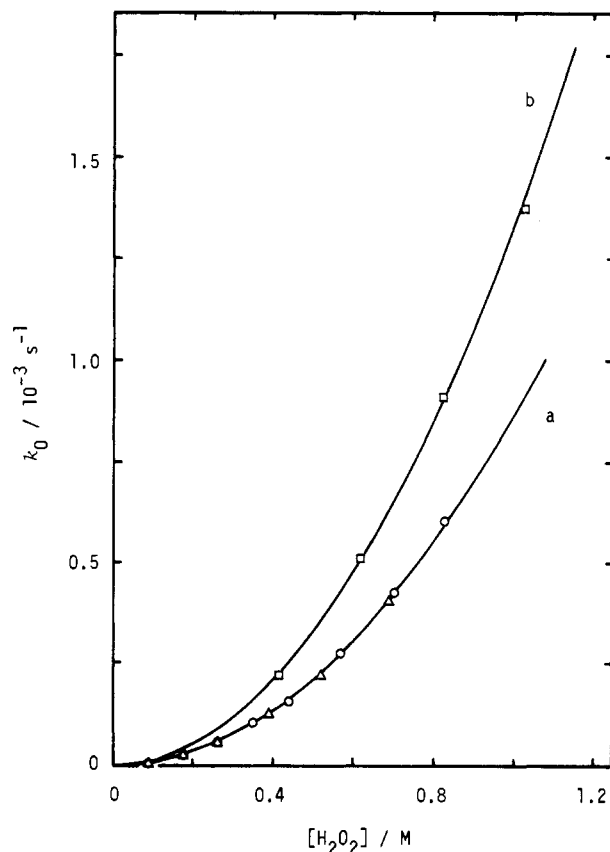
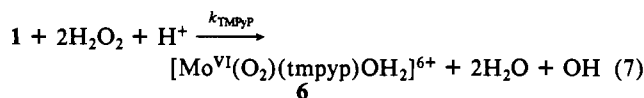


Figure 8. Dependence of the first-order rate constant, k_0 , of reaction 7 or 10 on the concentration of hydrogen peroxide at 35 °C: (a) for the TMPyP system at $[H^+] \approx 9.74 \times 10^{-3} \text{ M}$ (O) and $[H^+] = 9.74 \times 10^{-2} \text{ M}$ (Δ); (b) for the TPyP system at $[H^+] = 9.74 \times 10^{-3} \text{ M}$ (\square).

0.01–0.1 M. From the temperature and pressure dependence of the rate constants, activation parameters were estimated as given in Table II. In these processes hydrogen peroxide plays two roles, namely as an agent oxidizing molybdenum(V) to molybdenum(VI) and as a ligand that displaces either an oxo group or a coordinated water molecule at the axial site of the metalloporphyrin.

When the pH of the acidic solution of the reaction product (6) is raised by addition of an NaOH solution in the presence of a large excess of hydrogen peroxide, we observe the change in visible absorption spectra (ref to the spectra of 6 and 7 in Figure 3, where 7 is a product after the pH raise). Apparent molar absorption coefficients of the solution at various pHs are plotted as a function of $-\log[H^+]$ in Figure 9. The solid line in Figure 9 was calculated by using the conditional formation constant, $K'_{\text{Mo(VI)}} = [7][H^+]^2[6]^{-1}$. Values of $K'_{\text{Mo(VI)}}$ at 25 °C are $(2.2 \pm 0.2) \times 10^{-9}$ and $(4.8 \pm 0.4) \times 10^{-9} \text{ M}^2$ at $[\text{H}_2\text{O}_2] = 0.295$ and 0.739 M , respectively. The $K'_{\text{Mo(VI)}}$ values are proportional to $[\text{H}_2\text{O}_2]$. The consumption of 1 equiv of hydrogen peroxide and the release of two protons in the latter process clearly point to the coordination of a water molecule at the axial site of 6. Therefore, the reaction involving both the oxidation and the substitution may be described by eq 7. The free radical produced, OH, should be consumed



by the fast reaction with hydrogen peroxide present in large excess over the molybdenum complex.¹⁷ The change in absorption spectra over the pH range 3–5 corresponds to the substitution of the coordinated water molecule in 6 by hydrogen peroxide, pro-

(16) The following equations were used together with eq 5 for the evaluation of K_D value: $C_{\text{Mo(V)-TMPyP}} = (1 + K_{a1}[H^+])^{-1}[1] + 2K_{a1}^2K_D[H^+]^{-2}[1]^2$; $K_{a1} = [2][H^+][1]^{-1}$; $K_D = [3][2]^{-2}$.

(17) Funahashi, S.; Funada, S.; Inamo, M.; Kurita, R.; Tanaka, M. *Inorg. Chem.* **1982**, *21*, 2202. The second-order rate constant for the OH + H_2O_2 reaction is $4.5 \times 10^7 \text{ M}^{-1} \text{ s}^{-1}$; Field, R. J.; Noyes, R. M.; Postlethwaite, D. J. *Phys. Chem.* **1976**, *80*, 223.

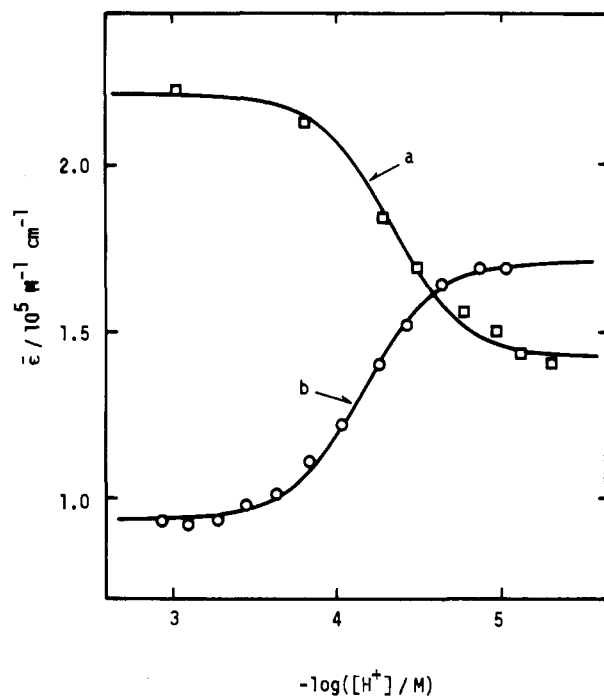
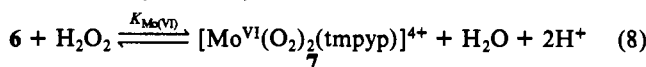


Figure 9. Plots of ϵ vs. $-\log([H^+]/M)$: (a) $[H_2O_2] = 0.295$ M at 443 nm; (b) $[H_2O_2] = 0.793$ M at 455 nm. Solid lines are calculated by using the obtained values of $K'_{Mo(V)}$ and molar absorption coefficients of **6** and **7** for each wavelength.

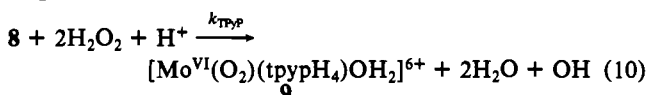
ducing diperoxomolybdenum(VI) porphyrin, $[Mo^{VI}(O_2)_2(tmpyp)]^{4+}$ (**7**). This process is written in eq 8. The equilibrium constant, defined as $K_{Mo(VI)} = [7][H^+]^2[6]^{-1}[H_2O_2]^{-1}$, was determined as $(6.9 \pm 0.5) \times 10^{-9}$ M at 25 °C.



Reaction of the Mo(V)–TPyP Complex with H_2O_2 in Acidic Aqueous Solutions. The Mo(V)–TPyP complex is soluble only in acidic aqueous solutions. Judging from the equilibria of the Mo(V)–TMPyP complex, the Mo(V)–TPyP complex is thought to exist as $[Mo^V O(tpypH_4)OH_2]^{5+}$ (**8**) in the acidic solution, where $tpypH_4$ represents the TPyP ligand of which four pyridyl groups are all protonated. Reactions with hydrogen peroxide were monitored over the pH range 1–3 in the same manner as for the Mo(V)–TMPyP system. The reaction is first order with respect to the concentration of **8**. Dependence of the first-order rate constant, k_0 , on the concentration of hydrogen peroxide is shown in Figure 8. The rate law is written by eq 9, similar to eq 6. This

$$-d[8]/dt = k_{TPyP}[8][H_2O_2]^2 \quad (9)$$

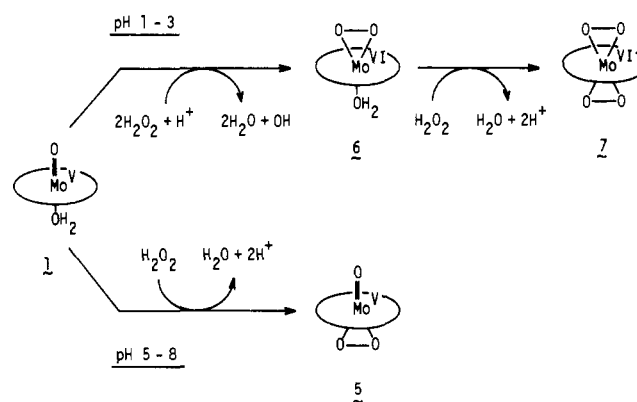
reaction is thus expressed as eq 10. The third-order rate constant k_{TPyP} and the corresponding activation parameters were obtained as given in Table II.



Discussion

According to recent structural studies, molybdenum(V) porphyrin complexes are either hexacoordinated monomers or hexa- or heptacoordinated dimers in the solid state and in aprotic solvents.^{11,12,18,19} The equilibrium network of the Mo(V)–TMPyP

Scheme II



complex as depicted in Scheme I involves very unique species such as dihydroxo-bridged and oxo-hydroxo-bridged dimeric species (**3** and **4**, respectively). Similar heptacoordinated dichloro-bridged or dialkoxo-bridged dimers have been reported.^{12,19}

Species **3** was found to dissociate to monomeric species (eq 4). The observed rate law points to a rapid preequilibrium protonation of the bridged ligand, followed by the rate-determining decomposition of the protonated dimer. Over the pH range from 4 to 9 the oxo-bridged dimeric iron(III) porphyrins dissociate according to the eq 11 and 12,²⁰ where P denotes a porphyrin such as TMPyP



or TPPS⁷ and K is defined as $K = [PFe-OH-FeP][H^+]^{-1}[PFe-O-FeP]^{-1}$. The rate law is expressed as eq 13. The values of rate =

$$kK[H^+](1 + K[H^+])^{-1}([PFe-O-FeP] + [PFe-OH-FeP]) \quad (13)$$

K and k are reported to be 7.52×10^5 M⁻¹ and 1.55×10^{-1} s⁻¹, respectively, for the TMPyP system. At $[H^+] \ll K^{-1}$, the first-order rate constant, $kK[H^+](1 + K[H^+])^{-1}$, can be approximated to $kK[H^+]$ just as for the dissociation of the dimeric Mo(V)–TMPyP complex, **3**. Second-order rate constants are similar for the two cases: $kK = 1.17 \times 10^5$ M⁻¹ s⁻¹ for the Fe(III)–TMPyP complex and $k_d = 4.1 \times 10^4$ M⁻¹ s⁻¹ for the Mo(V)–TMPyP complex.

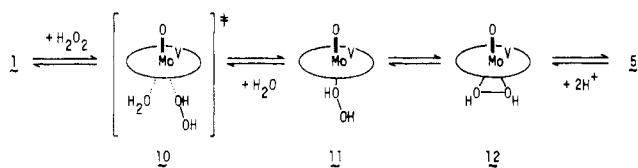
The reaction of the molybdenum(V) porphyrin complex with hydrogen peroxide has been known to produce diperoxomolybdenum(VI) porphyrin in aprotic solvents,³ while in aqueous solutions the TMPyP system involves three species of peroxomolybdenum porphyrins (**5**–**7**). The Mo(V)–TMPyP complex exists as an equilibrium mixture of four species (**1**–**4**), of which species **1** is the sole species reacting with hydrogen peroxide under the present conditions, as shown in Scheme II. The oxidizing power of hydrogen peroxide decreases with increasing pH. This is a reason why the oxidation of the molybdenum(V) to molybdenum(VI) by hydrogen peroxide occurs only in the acidic aqueous solution.

The reaction of the molybdenum(V) complexes with hydrogen peroxide in the acidic aqueous solution given by eq 7 and 10 involves the oxidation of the central metal ion as well as the substitution of an oxo group by a peroxy at the axial site of the complex. These two reactions cannot be observed separately in the present system, and we observe the second-order hydrogen peroxide dependence of the formation rate of **6** and **9**. Thus, one of two processes is thought to be a preequilibrium prior to the rate-determining step. Though the reduction of hydrogen peroxide needs a proton to give a hydroxyl radical and a water molecule ($H_2O_2 + H^+ + e^- \rightarrow OH + H_2O$) in the acidic aqueous solution, the overall rate is independent of hydrogen ion concentration (see

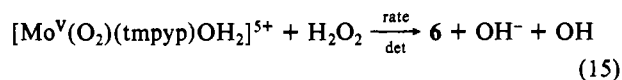
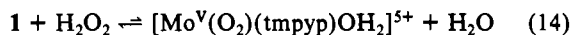
(18) Buchler, J. W.; Eickelmann, G.; Puppe, L.; Rohbock, K.; Schneehage, H. H.; Weck, D. *Justus Liebig's Ann. Chem.* **1971**, *745*, 135. Buchler, J. W.; Rohbock, K. *Inorg. Nucl. Chem. Lett.* **1972**, *8*, 1073. Buchler, J. W.; Puppe, L.; Rohbock, K.; Schneehage, H. H. *Ann. N.Y. Acad. Sci.* **1973**, *206*, 116. *Chem. Ber.* **1973**, *106*, 2710. Johnson, J. F.; Scheidt, W. R. *J. Am. Chem. Soc.* **1977**, *99*, 294. *Inorg. Chem.* **1978**, *17*, 1280. Hayes, R. G.; Scheidt, W. R. *Inorg. Chem.* **1978**, *17*, 1082. Ledon, H.; Mentzen, B. *Inorg. Chim. Acta* **1978**, *31*, L393.

(19) Matsuda, Y.; Yamada, S.; Murakami, Y. *Inorg. Chem.* **1981**, *20*, 2239.

Scheme III



eq 6 and 9). We thus conclude that the substitution of an oxo group in **1** and **8** by hydrogen peroxide should be the preequilibrium step and that the oxidation is rate determining. In the case of the TMPyP complex, we can write



Analogous reaction processes should be relevant to the Mo(V)–TPyP complex. As apparent from Table II, the activation parameters for k_{TMPyP} and k_{TPyP} are similar. Product **6** still has a coordinated water molecule. The substitution of this water molecule by another hydrogen peroxide gives diperoxomolybdenum(VI) porphyrin, **7** (eq 8). The geometry of the primary coordination sphere of **7** is presumed to be similar to that of $\text{Mo}^{\text{VI}}(\text{O}_2)_2(\text{tptp})$ where molybdenum is octacoordinated with four oxygen atoms of two peroxo groups and with four nitrogen atoms of the porphyrin.³ Interestingly, the diperoxomolybdenum(VI) porphyrin is produced directly by the reaction of the corresponding molybdenum(V) porphyrin with hydrogen peroxide in such aprotic solvent as dichloromethane,³ while in the aqueous solution we observe monoperoxomolybdenum(VI) porphyrin **6** as an intermediate.

On the other hand, the reaction of **1** with hydrogen peroxide in the neutral aqueous solution corresponds to the substitution of a coordinated water molecule at the axial site of **1** (eq 2). Judging from the equilibrium constant $K_{\text{Mo(V)}}$ it is reasonable that this reaction does not practically proceed in the acidic aqueous solution ($-\log [\text{H}^+] < 3$).

Activation volume is very useful in diagnosing the reaction mechanism. The measured volume of activation ΔV^\ddagger can be expressed as the sum of an intrinsic part $\Delta V_{\text{intr}}^\ddagger$ and an electrostatic part $\Delta V_{\text{el}}^\ddagger$.²¹ $\Delta V_{\text{intr}}^\ddagger$ represents the contribution to ΔV^\ddagger arising from the alteration of bond lengths and angles during the formation of the transition state, while $\Delta V_{\text{el}}^\ddagger$ reflects the variation in solvation. Activation volumes of the forward and reverse reactions of eq 2 are $\Delta V_f^\ddagger = -0.2 \pm 0.3 \text{ cm}^3 \text{ mol}^{-1}$ and $\Delta V_b^\ddagger = 5.2 \pm 1.6 \text{ cm}^3 \text{ mol}^{-1}$, respectively, and thus the reaction volume (ΔV) of reaction 2 is $-5.4 \pm 1.6 \text{ cm}^3 \text{ mol}^{-1}$. Since in the forward reaction hydrogen peroxide should attack the molybdenum(V) in **1** as a neutral form of H_2O_2 , there seems to be little or no

contribution of volume change due to solvation in the transition state. Therefore, the activation process of the peroxo complex formation is thought to be an interchange mechanism, where the increase in volume due to lengthening of the Mo–OH₂ bond in the transition state is almost compensated by the penetration of hydrogen peroxide into the inner coordination sphere of the central molybdenum(V) ion. We thus propose **10** as the transition state of this reaction as shown in Scheme III.

On the other hand, the course of the transition state in the reverse reaction is thought to involve the addition of two protons to the coordinated peroxo group of **5** to give intermediate **11** with hydrogen peroxide as a monodentate and the penetration of a water molecule into the inner coordination sphere of **11**. The latter process is considered as the rate-determining step of the reverse reaction and should be activated by an interchange mode as is the forward reaction. So, its activation volume is expected to be almost the same value (about $0 \text{ cm}^3 \text{ mol}^{-1}$) as that for the forward reaction. The volume change for the production of **11** is considered to result from the following three phenomena: (1) release of the electrostriction of two protons, for which the volume change is estimated to be ca. $9.0 \text{ cm}^3 \text{ mol}^{-1}$,²² (2) electrostriction associated with the increase of the total charge of the complex by the protonation of **5**, and (3) change of coordination mode of hydrogen peroxide from a bidentate in **12** to a monodentate in **11**. The third process seems to produce the volume increase corresponding to the difference between the partial molar volume of hydrogen peroxide and that of water, i.e., $5.7 \text{ cm}^3 \text{ mol}^{-1}$.²³ Thus, with a knowledge of $\Delta V_b^\ddagger = 5.2 \text{ cm}^3 \text{ mol}^{-1}$ we can estimate the volume change for the second phenomenon to be $-9.5 \text{ cm}^3 \text{ mol}^{-1}$. It is reasonable that this value is close to the difference in the partial molar volumes of **1** and **5**, i.e., $-9.3 \text{ cm}^3 \text{ mol}^{-1}$.²³

Acknowledgment. The authors thank Dr. Ryuichi Ikeda of the Faculty of Science, Nagoya University, for performing the ESR measurements. S.F. gratefully acknowledges financial support by a grant from the Kurata Foundation. Financial support from the Ministry of Education, Science, and Culture through a Grant-in-Aid for Scientific Research (Grant No. 59430010) is gratefully acknowledged.

Registry No. **1**, 95527-40-5; **2**, 96503-80-9; **2-4I**, 95527-35-8; **3**, 96503-81-0; **4**, 96503-82-1; **5**, 95527-37-0; **6**, 95527-38-1; **7**, 95527-39-2; $\text{Mo}^{\text{V}}\text{O}(\text{tmpyp})\text{OH}$, 95527-36-9; $\text{Mo}^{\text{V}}\text{O}(\text{tmpyp})^{5+}$, 96503-83-2; H_2O_2 , 7722-84-1.

Supplementary Material Available: Figure S1 giving ESR spectra of the Mo(V)–TMPyP complex, **1**, in acidic aqueous solution ($[\text{H}^+] = 1 \text{ M}$) (a) and of the peroxo complex **5** in aqueous solution (b) and Figure S2 giving plots of apparent molar absorption coefficients at 455 nm of the **1** solutions in the presence of various amounts of hydrogen peroxide vs. $\log ([\text{H}_2\text{O}_2]/\text{M})$ [$-\log ([\text{H}^+]/\text{M}) = 5.533$, $C_{\text{MES}} = 4.14 \times 10^{-3} \text{ M}$, 25°C] [inset: values of $\log (K'_{\text{Mo(V)}}/\text{M}^{-1})$ plotted against $-\log ([\text{H}^+]/\text{M})$] (2 pages). Ordering information is given on any current masthead page.

(20) Fleischer, E. B.; Palmer, J. M.; Srivastava, T. S.; Chatterjee, A. *J. Am. Chem. Soc.* **1971**, *93*, 3162. Pasternack, R. F.; Lee, H.; Malek, P.; Spencer, C. *J. Inorg. Nucl. Chem.* **1977**, *39*, 1865. Harris, F. L.; Toppen, D. L. *Inorg. Chem.* **1978**, *17*, 71.

(21) Swaddle, T. W. *Coord. Chem. Rev.* **1974**, *14*, 217.

(22) $\bar{V}(\text{H}^+) = -4.5 \text{ cm}^3 \text{ mol}^{-1}$: Palmer, D. A.; Kelm, H. *Inorg. Chem.* **1977**, *16*, 3139. Millero, F. J. *Chem. Rev.* **1971**, *71*, 147.

(23) The reaction volume of equilibrium 2, i.e., $\Delta V_f^\ddagger - \Delta V_b^\ddagger$, is expressed as $\bar{V}(\mathbf{5}) + \bar{V}(\text{H}_2\text{O}) + 2\bar{V}(\text{H}^+) - [\bar{V}(\mathbf{1}) + \bar{V}(\text{H}_2\text{O}_2)]$. With the values $\bar{V}(\text{H}_2\text{O}) = 18.0 \text{ cm}^3 \text{ mol}^{-1}$, $\bar{V}(\text{H}^+) = -4.5 \text{ cm}^3 \text{ mol}^{-1}$, and $\bar{V}(\text{H}_2\text{O}_2) = 23.7 \text{ cm}^3 \text{ mol}^{-1}$, we obtain the difference of the partial molar volume between **5** and **1**, $\bar{V}(\mathbf{5}) - \bar{V}(\mathbf{1})$, to be $9.3 \text{ cm}^3 \text{ mol}^{-1}$.